RSC Advances

REVIEW

View Article Online
View Journal | View Issue

Check for updates

Cite this: *RSC Adv.*, 2026, **16**, 11855

Water-dispersible perovskite nanocrystals: synthesis strategies, ion sensing applications, and future prospects

Zhixuan Lu, * Xinhua Weng, Jiayi Yang and Huan Fan

Perovskite nanocrystals (PeNCs) exhibit excellent optoelectronic properties including high quantum yield and tunable bandgap, making them promising for fluorescent sensing. However, their water sensitivity limits aqueous-phase applications. This review provides a critical analysis of strategies for preparing water-dispersible PeNCs, with a focused comparison between inorganic silica coating and organic polymer encapsulation in terms of their stability enhancement mechanisms, optical preservation, and ion permeability. We further explore applications in fluorescence-based ion sensing. Halide ions (Cl^-, I^-) are detected *via* anion-exchange chemistry, while metal cations (*e.g.*, Pb^{2+}, Cs^+, Fe^{3+}, Hg^{2+}, Cu^{2+}) are sensed through the fluorescence quenching effect or ion-triggered crystallization. The structure–property–performance relationships governing sensing selectivity and sensitivity are analyzed, highlighting the essential balance between environmental stability and controlled ion accessibility. Beyond summarizing recent advances, this review outlines current challenges and future prospects toward multiplexed detection, point-of-care devices, and bioimaging, providing a roadmap for the rational design and practical deployment of PeNCs in next-generation aqueous sensing platforms.

Received 13th December 2025
Accepted 26th February 2026

DOI: 10.1039/d5ra09645f

rsc.li/rsc-advances

Open Access Article. Published on 02 March 2026. Downloaded on 5/3/2026 3:03:50 PM.
This article is licensed under a Creative Commons Attribution-NonCommercial 3.0 Unported Licence.

Xiamen Key Laboratory of Optoelectronic Materials and Advanced Manufacturing, Institute of Luminescent Materials and Information Displays, College of Materials Science and Engineering, Huaqiao University, Xiamen 361021, China. E-mail: zxlu@hqu.edu.cn

Zhixuan Lu

Dr Zhixuan Lu is a Postdoctoral Fellow at Huaqiao University. He earned his PhD in Science under the supervision of Prof Bin Ren at Xiamen University. Currently, he works in the research group of Prof Zhanhua Wei at the Institute of Luminescent Materials and Information Displays, Huaqiao University. He has 20 publications in reputable international journals, with total citations exceeding 1300. He has also secured funding from the National Natural Science Foundation of China and the China Postdoctoral Science Foundation. His research primarily focuses on perovskite luminescent materials and their applications in fluorescent sensing and light-emitting diodes.

1. Introduction

Perovskite nanocrystals (PeNCs) have emerged as a prominent class of luminescent materials due to their exceptional optoelectronic properties, including high photoluminescence quantum yields (PLQYs), narrow emission bandwidths, and composition-tunable emission across the visible spectrum.[1,2] These attributes render them highly attractive for applications in photovoltaics,[1,3] light-emitting devices,[4,5] photodetectors,[6,7] and notably, fluorescent sensing and imaging.[8,9] For sensing applications, their high PLQY ensures bright signal output, while their tunable, narrow emission facilitates multiplexed detection schemes.[10]

However, the practical deployment of PeNCs in aqueous-based sensing is hindered by their intrinsic instability. Their ionic lattice and low formation energy make them highly susceptible to degradation by moisture, oxygen, and polar solvents.[11] Conventionally synthesized using long-chain organic ligands (*e.g.*, oleic acid and oleylamine) in nonpolar media, PeNCs are inherently hydrophobic.[12] Furthermore, ligand desorption during processing often leads to aggregation and loss of optical properties,[13,14] severely limiting their use in water-rich environments.

Consequently, developing robust strategies to impart water dispersibility and stability to PeNCs is paramount for unlocking their potential in chemical sensing. While several reviews have touched upon perovskite stability or sensing applications separately,[15–17] a systematic analysis focusing on how different

© 2026 The Author(s). Published by the Royal Society of Chemistry

Open Access Article. Published on 02 March 2026. Downloaded on 5/3/2026 3:03:50 PM. This article is licensed under a Creative Commons Attribution-NonCommercial 3.0 Unported Licence.

encapsulation strategies directly enable and modulate ion sensing performance in water is still needed. This review aims to fill this gap by critically summarizing recent advances in the preparation of water-dispersible PeNCs, with a focused comparison between two dominant approaches: encapsulation within inorganic silica (SiO_2) matrices and organic polymers. We evaluate their respective merits and limitations in conferring water stability, preserving fluorescence, and permitting controlled ion access—the triad essential for sensing. Furthermore, we provide a comprehensive discussion on the burgeoning applications of these stabilized PeNCs in the fluorescence-based detection of ions, categorizing them into halide and metal ion sensing. We delve into the underlying mechanisms (anion exchange, quenching, *in situ* formation) and highlight the critical structure–property–sensitivity relationships. Finally, we outline the persistent challenges in selectivity, biocompatibility, and device integration, and propose future directions toward multiplexed sensing, point-of-care diagnostics, and bioimaging. This review is intended to provide a timely and critical perspective for researchers aiming to leverage the outstanding optical properties of perovskites in aqueous environments for next-generation sensing platforms.

2. Preparation of water-dispersible PeNCs

2.1. Inorganic silica encapsulation

Encapsulation within inorganic matrices represents a widely adopted approach to confer water compatibility and environmental robustness to nanocrystals. A dense SiO_2 shell acts as a physical and chemical barrier that shields the ionic perovskite core from hydrolytic attack while preventing particle aggregation. The sol–gel process, typically using alkoxysilane precursors like tetraethyl orthosilicate (TEOS) or tetramethyl orthosilicate (TMOS), allows for relatively good control over shell thickness and morphology. An effective silica coating must be conformal and defect-free to maximize protection, yet it should not completely isolate the PeNC core if ion exchange is the intended sensing mechanism.

As shown in Fig. 1a, Cynthia Collantes and co-workers presented a water-assisted synthesis of stable and multicolored $CsPbX_3@SiO_2$ core–shell nanoparticles through a transformative mechanism where Cs_4PbX_6 precursors are converted to luminescent $CsPbX_3$ NCs in the presence of partially hydrolyzed TMOS, simultaneously triggering silica shell formation.[18] The resulting particles exhibit tunable emission (490–700 nm), small size (<30 nm), enhanced PLQY (up to 60%), and improved moisture stability after thermal treatment, enabling their conjugation to antibodies for biosensing. $CsPbBr_3$ quantum dots were grown *in situ* within the radial mesopores of core–shell silica microspheres (CSSM).[19] Subsequent pore sealing with a hydrophobic agent (octadecyltrichlorosilane, ODS) provided exceptional water resistance. The CSSM-$CsPbBr_3$ composite retained >90% of its initial PL intensity after 30 days of water immersion—a benchmark for long-term silica-based stability. A core–shell synthesis was developed where maleic anhydride triggered the conversion of Cs_4PbBr_6 to $CsPbBr_3$ nanocrystals and subsequently promoted the uniform hydrolysis of TMOS to form a coherent ~15 nm silica shell around each ~9 nm core.[20] The encapsulated particles showed significantly improved aqueous stability over short-term testing. A dual-layer encapsulation strategy was employed. $CsPbBr_3$ NCs were first coated with silica *via* a ligand-assisted method and then encapsulated within PEGylated phospholipid (mPEG-DSPE) micelles (Fig. 1b).[21] This architecture conferred excellent aqueous stability, retaining >80% PL intensity after two weeks in water or buffers, alongside resistance to UV and ultrasonication. A "stress-response" encapsulation strategy was reported, where environmental moisture triggered the hydrolysis of (3-aminopropyl)triethoxysilane (APTES) to form a compact SiO_2 shell on individual $CsPbBr_3$ NCs.[22] The $CsPbBr_3@SiO_2$ nanoparticles maintained strong photoluminescence in water for over 48 hours, far exceeding the stability of uncoated NCs. As illustrated in Fig. 1c and a dual-passivation strategy utilized (3-iodopropyl)trimethoxysilane, which simultaneously provided iodine for surface defect passivation and hydrolyzed to form a conformal SiO_2 layer around $CsPbI_3$ NCs.[23] The core–shell nanoparticles demonstrated enhanced water stability and resistance to moisture-induced phase degradation for over 24 hours. The thickness and porosity of the silica shell are critical design parameters. Thinner, more porous shells (often achieved by controlling hydrolysis/condensation rates) favor ion permeability for faster sensing kinetics but may compromise long-term stability. Conversely, thicker, denser shells offer superior protection but can insulate the PeNC core, reducing sensitivity. Chemical functionality (*e.g.*, introducing amine groups *via* APTES) can enhance dispersion and provide sites for further conjugation or selective ion interaction.[24] While silica encapsulation offers significant advantages such as biocompatibility and facile surface functionalization, precise control over reaction kinetics is also crucial to prevent particle sintering and aggregation, which can compromise dispersibility and optical quality.

2.2. Organic polymer encapsulation

Organic polymer encapsulation provides a versatile alternative, equipping fragile PeNCs with a multifunctional protective layer. This strategy not only offers a robust barrier against water and oxygen but can also passivate surface defects, suppress ion migration, and introduce hydrophilic or bioactive groups for dispersion in complex media.[25] Polymers can be employed as dense shells, embedding matrices, or amphiphilic micelles/vesicles.

An *in situ* hot-injection method was used to embed $CsPbX_3$ NCs into carboxyl-functionalized PMMA spheres.[26] The swelling-shrinking behavior of PMMA during synthesis effectively caps the NCs, granting water resistance (90% PL retention after 12 hours in water) and suppressing anion exchange. $CsPbBr_3$ NCs were embedded into polyethylene glycol-polycaprolactone (PEG-PCL) *block* copolymer micelles *via* a dispersion-precipitation-redispersion method.[27] The hydrophobic PCL core shielded the NCs, while the hydrophilic PEG

© 2026 The Author(s). Published by the Royal Society of Chemistry

Open Access Article. Published on 02 March 2026. Downloaded on 5/3/2026 3:03:50 PM.
This article is licensed under a Creative Commons Attribution-NonCommercial 3.0 Unported Licence.

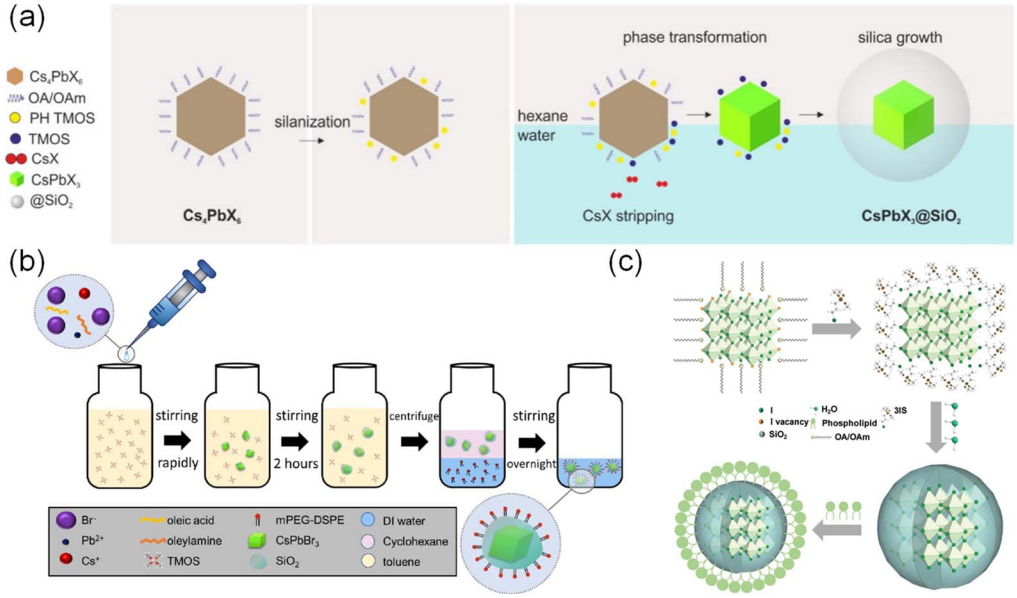

Fig. 1 (a) Scheme of the water-assisted synthesis of stable $CsPbX_3$@SiO_2 core–shell nanoparticles formation mechanism. Reproduced with permission from ref. 18. (b) Scheme of a SiO_2 layer on the $CsPbBr_3$ NCs and encapsulating the $CsPbBr_3$/SiO_2 NCs within PEGylated phospholipid micelles. Reproduced with permission from ref. 21. (c) Schematic diagram of the synthesis of $CsPbI_3$/3I@SiO_2 phospholipid micelles. Reproduced with permission from ref. 23.

corona ensured colloidal stability. The resulting "bio-PeNCs" retained 94% of their initial PLQY after 15 days in water and enabled long-term H_2S sensing in live cells and zebrafish. The NCs maintained their PLQY for 15 days in water, enabling cell imaging and biosensing. As shown in Fig. 2a, an automated, stepwise protocol encapsulated $CsPbBr_3$ NCs using polystyrene-*block*-poly(acrylic acid) (PS-*b*-PAA).[28] Solvent-driven self-assembly yielded capsules with a hydrophobic PS anchor and a hydrophilic PAA corona. These capsules exhibited remarkable long-term stability, maintaining ~60% PLQY in water for over two years, with robustness in various polar solvents and saline. Yamauchi *et al.* presented a template-based synthesis of porous polymers (Fig. 2b).[29] Water-soluble perovskite fluorides served as sacrificial templates for a solid-state Schiff-base reaction. Subsequent water washing removed the template, yielding meso-/macro-porous polymers with tunable pore sizes and hydrophilic surfaces. An aqueous, stepwise crystallization strategy was developed for *in situ* growth of $MAPbBr_3$ NCs within a PVA matrix.[30] A "fast drying–slow moistening" sequence decoupled polymer solidification from perovskite crystallization, allowing humidity-controlled tuning of optical properties and yielding films with a PLQY of 95.3%. A multi-strategy approach combined Mn^{2+} doping, core–shell heterostructure formation, and amphiphilic polymer encapsulation. Mn^{2+}-doped $CsPbCl_3$ NCs, capped with NH_2-PEG-COOH, underwent a water-triggered phase transition to form a protective $CsPb_2Cl_5$ shell.[31] Polymer design rules for ion sensing are multifaceted. The hydrophobicity/hydrophilicity balance of block copolymers dictates colloidal stability and water uptake. Cross-linking density within the polymer network controls swelling and analyte diffusion rates. Functional groups (*e.g.*, carboxyl, amine, thiol) can be incorporated to selectively chelate target metal ions, enhancing selectivity.[32] For instance, polymers rich in oxygen or nitrogen donors are favorable for sensing metal cations like Fe^{3+} or Cu^{2+} *via* coordination-induced quenching.[33–35] The molecular weight and architecture (linear, branched, dendritic) also influence the compactness of the protective layer and its permeability. Collectively, polymer-based strategies offer a versatile toolbox for rendering PeNCs water-compatible, providing tunable interfaces that address core stability challenges for sensing in complex aqueous environments.

2.3. Comparison of silica and polymer encapsulation strategies

The core challenge in aqueous sensing with PeNCs is to shield the ionic core from hydrolytic degradation while maintaining or even enhancing its optical properties and allowing selective interaction with target analytes. Encapsulation within a protective shell is the most effective strategy. The two primary material choices—inorganic silica and organic polymers—offer distinct advantages and trade-offs concerning barrier properties, permeability, surface functionality, and biocompatibility. As summarized in Table 1, silica coating and polymer encapsulation offer distinct physical and chemical profiles, leading to divergent trade-offs between stability, functionality, and ion accessibility.

Silica encapsulation typically results in shells with thicknesses ranging from 5 to 30 nm. Its principal strength lies in providing an excellent barrier against water and oxygen, coupled with high chemical and thermal stability. The surface hydroxyl groups facilitate further functionalization, enhancing compatibility with various sensing interfaces.[36] However, silica shells can be brittle and may impede ion diffusion, potentially

Open Access Article. Published on 02 March 2026. Downloaded on 5/3/2026 3:03:50 PM.
This article is licensed under a Creative Commons Attribution-NonCommercial 3.0 Unported Licence.

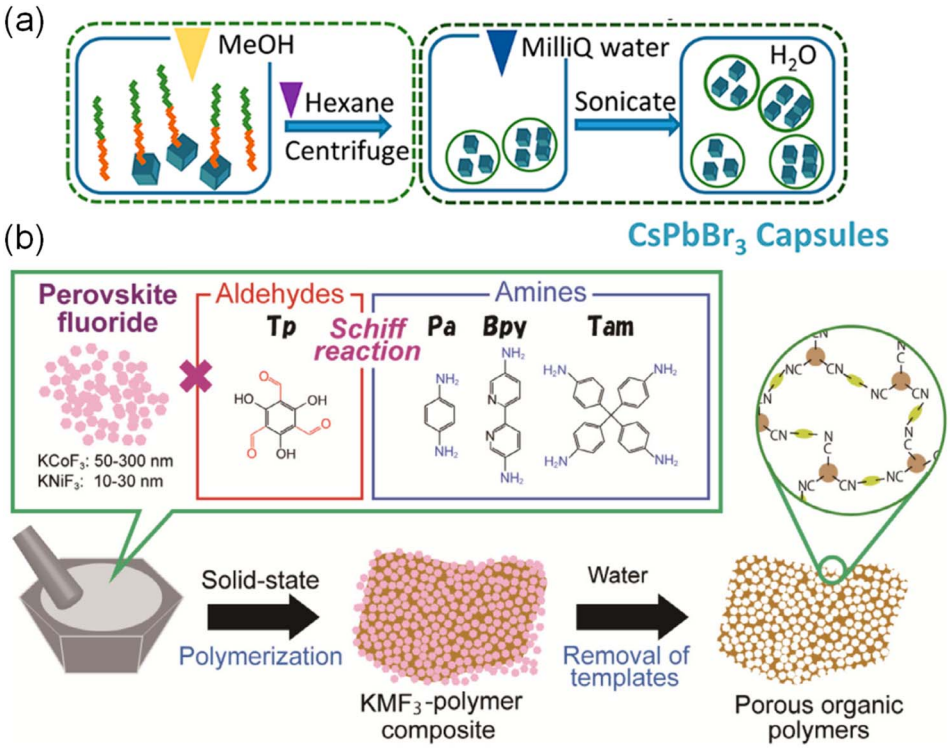

Fig. 2 (a) Schematic illustration of the room temperature process developed for the fabrication of the capsules embedding the $CsPbBr_3$ NCs. Reproduced with permission from ref. 28. (b) Formation of porous organic polymers by using perovskite fluorides as a water-soluble template. Reproduced with permission from ref. 29.

reducing sensing kinetics. Moreover, the sol–gel synthesis requires precise control to prevent nanoparticle aggregation. In terms of aqueous stability, silica-coated PeNCs can retain >80% photoluminescence for days to months, as exemplified by CSSM-$CsPbBr_3$ composites that remain stable over 30 days in water.[20] Ion permeability through silica is generally low to moderate, though it can be tuned by adjusting shell porosity and density. In contrast, polymer encapsulation offers greater versatility in shell architecture, with thicknesses spanning 2–50 nm or serving as an embedding matrix. Polymers provide high flexibility and processability, along with tunable permeability and surface functionality—key for designing selective sensing interfaces. They also exhibit good biocompatibility and can passivate surface defects on PeNCs. Limitations include possible swelling in certain solvents, variable long-term stability, and potential non-specific binding in complex media. Stability can range from hours to years; notably, PS-*b*-PAA encapsulated PeNCs maintain significant PL over two years in water.[29] Most importantly, ion permeability through polymer shells is highly tunable, from low to high, enabling tailored sensing responses.

The choice between silica and polymer encapsulation represents a deliberate compromise between competing material properties. Silica-based coatings prioritize long-term environmental robustness, though they may restrict ion access to the perovskite core. In contrast, polymer encapsulation emphasizes customizable interfacial properties and tunable permeability, making it better suited for dynamic sensing in aqueous or biological environments. Ultimately, the selection should be guided by the specific demands of the target ion-

Table 1 Comparison of silica and polymer encapsulation strategies for water-dispersible PeNCs

Strategy	Silica coating	Polymer encapsulation
Shell thickness	5–30 nm	2–50 nm (or matrix)
Advantages	Excellent barrier against H_2O/O_2; high chemical/thermal stability; facile surface –OH functionalization	High flexibility and processability; tunable permeability; good biocompatibility; can passivate surface defects
Limitations	Hinder ion diffusion; requires precise control to avoid aggregation during sol–gel process	Swell in solvents; potential for non-specific binding
Water stability (PL retention >80%)	Days to months (*e.g.*, >30 days for CSSM-$CsPbBr_3$)	Hours to years (*e.g.*, >2 years for PS-*b*-PAA capsules)
Ion permeability	Low to moderate; tunable *via* porosity/density	Highly tunable (low to high)

© 2026 The Author(s). Published by the Royal Society of Chemistry

Open Access Article. Published on 02 March 2026. Downloaded on 5/3/2026 3:03:50 PM. This article is licensed under a Creative Commons Attribution-NonCommercial 3.0 Unported Licence.

sensing application, particularly in terms of stability, sensitivity, and required operational duration.

3. Ion sensing based on water-dispersible PeNCs

The successful stabilization of PeNCs in water opens the door to exploiting their rich photophysical responses to ions. Sensing mechanisms can be broadly classified into two categories: (1) anion exchange, primarily for halides, which modulates the bandgap and emission color, and (2) fluorescence quenching or enhancement, often for metal cations, through electron transfer, energy transfer, or ion-triggered structural changes.

3.1. Halide ion sensing

The intrinsic incorporation of halide ions into the perovskite lattice, combined with their direct influence on the emission wavelength of perovskite nanocrystals, establishes a unique and robust foundation for fluorescence-based halide sensing. This inherent structure–property relationship facilitates sensitive detection *via* spectroscopically distinguishable anion-exchange reactions.

For example, $CsPbBr_3$ PNCs in *n*-hexane were used for Cl^- detection *via* rapid interfacial anion exchange during vortex mixing, causing an emission blueshift.[37] A linear range of 10–200 μM and a limit of detection (LOD) of 4 μM were achieved. Chen *et al.* found that halide sensing can occur at water–oil interfaces (Fig. 3b).[38] Organic iodides facilitated I^- exchange, inducing a measurable PL redshift with high sensitivity (LOD: 0.2 nmol L^{-1}). $CsPbBr_3$ NCs stabilized in a β-cyclodextrin/arginine network within ethanol–water mixtures detected Cl^- and I^- *via* characteristic emission shifts, offering visual colorimetric response with μM-level LODs.[39] Using a two-phase hexane-water system, Cl^- detection *via* interfacial exchange enabled rapid (<5 min) on-site quantification with ~99% accuracy in wastewater using a portable device.[40] As shown in Fig. 3a, $CsPbBr_3$ NCs coated with a thin, halide-permeable silicone layer *via* (3-aminopropyl)trimethoxysilane (APTMS) were used in a ternary solvent system.[41] Cl^- exchange caused a rapid blueshift with a linear range of 0.2–20 mM, and the material was processed into films for visual sweat analysis. As illustrated in Fig. 3c and a directly water-dispersible $CsPbBr_3$@$CsPb_2Br_5$ composite was synthesized.[42] It enabled the detection of Cl^- (blueshift) and I^- (redshift) *via* anion exchange, allowing for sensitive and smartphone-compatible visual quantification. Water-stable, oleylamine-capped $CsPbBr_3$ NCs prepared *via* dual supersaturation recrystallization detected I^- through an anion-exchange-induced redshift (LOD: 0.40 μM).[43] Mishra and co-workers employed hot-injection synthesized $CsPbBr_3$ PeNCs for Cl^- detection, leveraging a rapid anion-exchange mechanism where Cl^- ions replace Br^- in the PeNCs lattice, resulting in a pronounced blue shift in photoluminescence. The sensor demonstrated a detection limit as low as 100 μM and enabled visible colorimetric readout from green to blue under UV light, applicable in solution, film, and paper-based formats for on-site analysis.[44] The method exhibited high selectivity for Cl^- over other common ions, highlighting its potential as a simple, portable spectrochemical probe for environmental water monitoring (Table 2).

The key design principle for halide sensing is to balance stability with controlled permeability. The encapsulation shell must protect the core from dissolution but allow the target halide ions to reach the perovskite surface. This is often achieved by using thin, porous, or ionically conductive shells, or by creating local environments (like interfaces or micelles) where exchange can occur while bulk water is excluded. Collectively, these studies demonstrate that effective halide ion sensing with perovskite nanocrystals does not require perfect aqueous

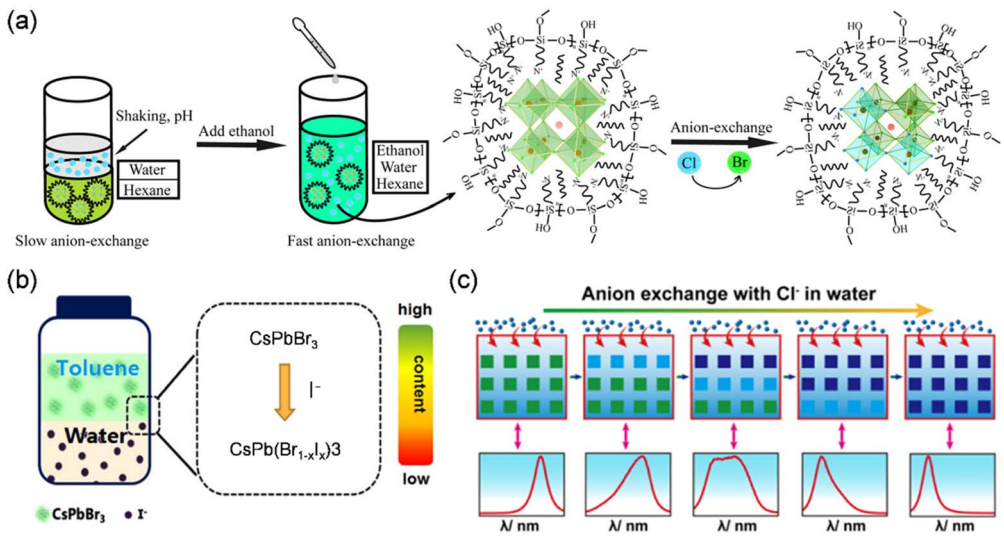

Fig. 3 (a) Fast anion-exchange of PeNCs in hexane with Cl^- in the aqueous phase. Reproduced with permission from ref. 41. (b) Schematic of the colorimetric sensing for the content of oxides in aqueous solution using PeNCs. Redrawn from ref. 38. (c) Dynamics of anion exchange between PeNCs and Cl^- in water. Reproduced with permission from ref. 42.

Open Access Article. Published on 02 March 2026. Downloaded on 5/3/2026 3:03:50 PM. This article is licensed under a Creative Commons Attribution-NonCommercial 3.0 Unported Licence.

Table 2 Performance summary of halide ion sensors based on water-dispersible PeNCs

Perovskite material	Target ion	Mechanism	LOD	Stability in water
$CsPbBr_3$ in hexane[37]	Cl^-	Interfacial anion exchange	4 μM	N/A
$CsPbBr_3$@β-CD/Arg[39]	Cl^-, I^-	Anion exchange in mixed solvent	μM level	Good in EtOH/H_2O
Silicone-coated $CsPbBr_3$ (ref. 41)	Cl^-	Permeable shell anion exchange	2.66 mM	Good in solvent
$CsPbBr_3$@$CsPb_2Br_5$ (ref. 42)	Cl^-, I^-	Anion exchange	3.2 μM	>24 h
Oleylamine-capped $CsPbBr_3$ (ref. 43)	I^-	Anion exchange	0.40 μM	Stable

solubility. Instead, it hinges on the creation of a stable interface or matrix that permits controlled halide exchange while protecting the perovskite core. The prevailing strategy involves a careful trade-off between providing sufficient stability against degradation by bulk water and maintaining controlled ion permeability or access to the nanocrystal surface. Achieving this balance is crucial for transforming the inherent halide sensitivity of perovskite materials into a reliable and quantitative sensing mechanism suitable for environmental and biological applications.

3.2. Metal ion sensing

The optical properties of PeNCs exhibit a pronounced susceptibility not only to halide ions but also to a diverse array of metal cations. Metal ion detection using PeNCs primarily relies on fluorescence quenching (or less commonly, enhancement) caused by interactions between the cation and the nanocrystal surface or its encapsulating layer. Mechanisms include static quenching *via* coordination, dynamic quenching *via* electron/energy transfer, or ion-triggered structural transformation of the perovskite itself. This inherent responsiveness forms the foundational principle for designing PeNC-based fluorescent probes for the quantitative detection of these ions. The underlying sensing mechanisms extend beyond simple ion exchange to encompass ion-triggered *in situ* perovskite formation and selective fluorescence quenching.

For instance, a particularly rapid detection method for Pb^{2+} was enabled by the *in situ* formation of $FAPbI_3$ perovskite.[45] As illustrated in Fig. 4b, in this approach, a formamidinium iodide solution reacts instantly with aqueous Pb^{2+} to form fluorescent $FAPbI_3$. The associated bandgap reduction leads to emission quenching, allowing for visual detection within three seconds. This method achieves aLOD of 100 nM across a broad linear range from 100 nM to 1 mM with high selectivity for Pb^{2+}. For the detection of Cs^+, a hybrid ionic liquid membrane strategy was presented (Fig. 4a).[46] A membrane impregnated with a Pb/Br-containing ionic liquid forms fluorescent $CsPbBr_3$ NCs *in situ* upon contact with aqueous Cs^+. This yields a selective green emission under UV light, even in high-salinity environments, with a LOD of 0.18 mg L^{-1}, a visual readout time under one minute, and ultra-low cost. A modified swelling-shrinking strategy was employed to encapsulate $CsPbBr_3$ quantum dots within poly(styrene/acrylamide) nanospheres, resulting in hyperstable, water-dispersible fluorescent beads.[47] These beads function as a probe for Fe^{3+} *via* static fluorescence quenching, which is initiated by chelation between the target ions and surface carboxyl groups. This system demonstrates high selectivity, a linear detection range from 5 to 150 μM, and a LOD of 2.2 μM in complex matrices such as river water and serum. Similarly, a sandwich-structured SiO_2@$CsPbX_3$@SiO_2 composite was fabricated to ensure aqueous stability for sensing applications.[48] The detection of Fe^{3+} ions by this composite relies on chelation-induced fluorescence quenching with surface oxygen-containing groups, offering a linear range

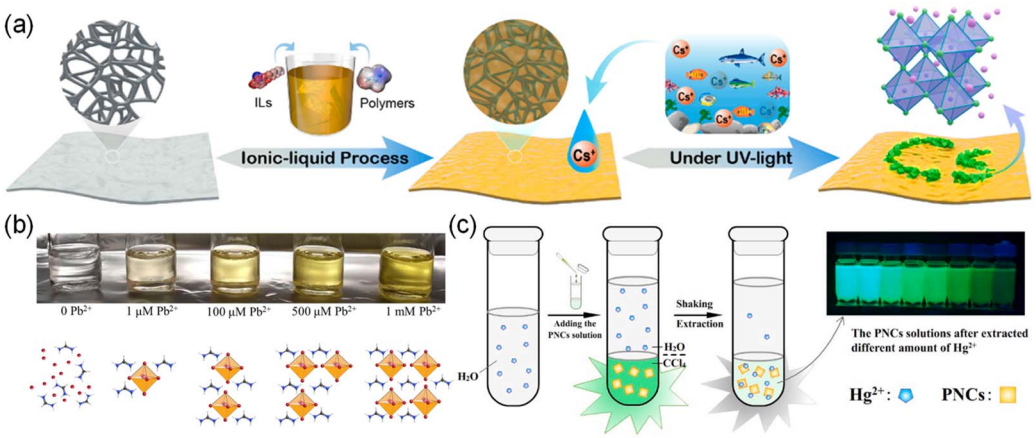

Fig. 4 (a) Schematics detection of cesium ion in seawater *via* PeNCs fluorescence. Reproduced with permission from ref. 46. (b) Schematic representation of the formation of PeNCs with the corresponding concentrations of Pb^{2+}. Reproduced with permission from ref. 45. (c) Illustration of liquid–liquid extraction and visual detection of Hg^{2+} using PeNCs. Reproduced with permission from ref. 49.

© 2026 The Author(s). Published by the Royal Society of Chemistry

Open Access Article. Published on 02 March 2026. Downloaded on 5/3/2026 3:03:50 PM. This article is licensed under a Creative Commons Attribution-NonCommercial 3.0 Unported Licence.

Table 3 Performance summary of metal ion sensors based on water-dispersible PeNCs

Perovskite material	Target ion	Mechanism	LOD	Key feature
In situ formed $FAPbI_3$ (ref. 45)	Pb^{2+}	Ion-triggered crystallization	100 nM	Visual
Perovskite precursor[46]	Cs^+	*In situ* formation of $CsPbBr_3$	0.18 mg L^{-1}	In high salinity
$CsPbBr_3$@PS-Am beads[47]	Fe^{3+}	Chelation-induced quenching	2.2 μM	Selectivity in serum
SiO_2@$CsPbX_3$@SiO_2 (ref. 48)	Fe^{3+}	Chelation-induced quenching	3 μM	Sandwich structure
$CsPbBr_3$ (ref. 49)	Hg^{2+}	Electron transfer quenching	35.65 μM	Liquid–liquid extraction
PVP/NIPAM capped $CsPbBr_3$ (ref. 50)	Cu^{2+}	Electron transfer quenching	18.6 μM	Thermo-responsive polymer

of 10–70 μM and a LOD of 3 μM in real water samples. As shown in Fig. 4a, a liquid–liquid extraction strategy for Hg^{2+} detection was described.[49] Here, $CsPbBr_3$ PNCs in a carbon tetrachloride phase extract Hg^{2+} from an aqueous medium. Fluorescence quenching occurs through an electron transfer or surface interaction mechanism induced by Hg^{2+}, which also shortens the photoluminescence lifetime. The method achieves a detection limit of 35.65 nM with a linear range of 50 nM to 10 μM and high selectivity, proving effective for the analysis of environmental waters. Water-dispersible $CsPbBr_3$ nanocrystals synthesized *via* a modified ligand-assisted reprecipitation method with polyvinyl-pyrrolidone/*N*-isopropyl acrylamide (PVP/NIPAM) encapsulation were reported.[50] These polymer-coated NCs act as a selective fluorescent probe for Cu^{2+} *via* an electron-transfer quenching mechanism, achieving a LOD of 18.6 μM while maintaining aqueous stability and optical properties. Furthermore, a lead-free sensing paradigm was demonstrated using a two-dimensional Pd(II)-based perovskite, $(C_4H_{16}N_3)[PdCl_4]Cl$. This material serves as an electrode modifier for the electrochemical detection of Zn^{2+} *via* catalytic oxidation in aqueous buffers.[51] While not a fluorescent aqueous probe, it exhibits high sensitivity with a detection limit of 20 nM, excellent selectivity, and reliable performance in real water samples (Table 3).

Based on the above, it can be concluded that metal-ion detection using PeNCs exploits diverse mechanisms including coordination chemistry, electron transfer, and ion-triggered crystallization. A central challenge in this field involves engineering the nanocrystal surface or its encapsulating matrix to concurrently ensure high stability in aqueous media and selective accessibility for the target metal ion. This requirement necessitates a careful design of the interfacial chemistry to promote specific interactions while mitigating non-specific quenching, underscoring the intricate balance between stability, selectivity, and sensitivity that defines advanced metal-ion sensing applications.

3.3. Interplay and coexistence of sensing mechanisms in complex media

In real-world samples (*e.g.*, environmental water, biological fluids), multiple ions coexist, potentially leading to interference.[52] The anion-exchange and quenching mechanisms may operate simultaneously or competitively. For instance, in a sample containing both Cl^- and Cu^{2+}, Cl^- might induce a blueshift while Cu^{2+} quenches the overall intensity, complicating signal interpretation. The encapsulation design dictates the dominant pathway. A dense, charge-selective shell might block multivalent metal ions but allow small halides, favoring anion-exchange sensing. Conversely, a polymer shell with chelating groups might preferentially bind and admit specific metal ions, making quenching the dominant response. Recent studies are exploring ratiometric or array-based sensing approaches to deconvolute such mixed signals.[53,54] Using two different PeNCs (*e.g.*, one sensitive to halides, one to a metal) within the same platform, or monitoring both emission wavelength and intensity changes, can provide multidimensional data for accurate analysis in complex matrices.

4. Conclusion and perspectives

This review has outlined the significant progress in stabilizing PeNCs for operation in aqueous environments, primarily through inorganic silica and organic polymer encapsulation strategies. These methods have successfully transformed the intrinsically water-sensitive PeNCs into robust, water-dispersible fluorescent probes, largely preserving their exceptional PLQYs and tunable emission. Leveraging these stabilized materials, researchers have developed sensitive fluorescence-based sensors for both halide and metal ions. Halide detection capitalizes on the intrinsic anion-exchange chemistry of perovskites, while metal-ion sensing exploits mechanisms such as selective quenching, ion-triggered crystallization, and catalytic reactions.

Despite these advances, the translation of laboratory demonstrations into real-world applications faces several persistent challenges. A primary concern is ensuring long-term stability under biologically or environmentally relevant conditions, as performance in complex media such as cell culture sera or samples with variable pH often remains inadequate compared to tests in pure water. Achieving high selectivity among interfering ions in complex matrices also requires significant improvement, necessitating the more effective integration of molecular recognition elements like aptamers, ionophores, or enzymes into the encapsulation design. Furthermore, the potential toxicity and biocompatibility issues, particularly lead leakage from Pb-based PeNCs, must be addressed through strategies such as developing hermetic seals, adopting lead-free perovskites, and conducting thorough cytotoxicity studies. For commercialization, achieving consistent batch-to-batch reproducibility in encapsulation quality and

Open Access Article. Published on 02 March 2026. Downloaded on 5/3/2026 3:03:50 PM. This article is licensed under a Creative Commons Attribution-NonCommercial 3.0 Unported Licence.

sensing performance is essential, calling for automated and scalable synthesis methods. Finally, a deeper mechanistic understanding of ion transport through protective shells and their interaction with the PeNCs surface in aqueous environments is needed, potentially advanced by *in situ* and *operando* spectroscopic or microscopic studies.

Looking ahead, the field is poised to advance in several promising directions. The tunable emission of PeNCs is ideally suited for multiplexed and multimodal sensing. This can be realized through strategies such as spatial patterning of different PeNCs, temporal coding, or developing ratiometric probes that combine a PeNC signal with a stable reference dye. Integrating fluorescence readout with other transduction mechanisms, like electrochemical,[55] could further enable robust multimodal sensors. Another direction involves processing stable PeNCs inks into films, hydrogels, or paper-based strips to fabricate low-cost, portable point-of-care and wearable devices. Their integration with smartphone cameras and LEDs presents a viable path toward field-deployable diagnostic tools. The bright and photostable luminescence of water-compatible PeNCs also makes them attractive probes for intracellular sensing and bioimaging, potentially allowing the monitoring of dynamic ion fluxes such as Ca^{2+}, Zn^{2+}, or pH in living cells, provided challenges in cellular delivery, subcellular targeting, and long-term biocompatibility are resolved. Moreover, future material designs may evolve beyond simple core–shell structures toward intelligent, stimuli-responsive systems—for instance, those activated by pH, enzymes, or light—or hierarchical architectures that synergistically combine silica and polymers.

In conclusion, the journey of rendering perovskites water-compatible has unlocked a new frontier for their application in analytical chemistry. By continuing to innovate at the intersection of materials chemistry, surface science, and device engineering, water-dispersible PeNCs are set to become a powerful and versatile tool in the next generation of optical sensors.

Conflicts of interest

The authors declare no conflicts of interest.

Data availability

No primary research results, software or code have been included and no new data were generated or analysed as part of this review.

Acknowledgements

The authors would like to thank the National Natural Science Foundation of China (NSFC) (52402186), the China Postdoctoral Science Foundation (2023M731164),the Open Research Project of State Key Laboratory of Physical Chemistry of Solid Surfaces of Xiamen University (202423), and Scientific Research Funds of Huaqiao University (22BS132) for financial support.

References

1 W. Yang, S. H. Jo and T. W. Lee, *Adv. Mater.*, 2024, **36**, 2401788.
2 Y. Wu, D. Chen, G. Zou, H. Liu, Z. Zhu, A. L. Rogach and H.-L. Yip, *ACS Nano*, 2025, **19**, 9740–9759.
3 M. K. Chini, *Energy Technol.*, 2024, **12**, 2301444.
4 Z. Lu, Y. Li, L. Wei, Y. Jiang, F. Yu, H. Fan, J. Yang, J. Xing and Z. Wei, *Chem. Eng. J.*, 2025, **519**, 165202.
5 Y. Shi, J. Yang and Z. Lu, *Photonics*, 2026, **13**, 151.
6 X. Li, S. Aftab, M. Mukhtar, F. Kabir, M. F. Khan, H. H. Hegazy and E. Akman, *Nano Micro Lett.*, 2025, **17**, 28.
7 Y. H. Lee, W. J. Lee, G. S. Lee, J. Y. Park, B. Yuan, Y. Won, J. Mun, H. Yang, S. D. Baek and H. Lee, *Adv. Mater.*, 2025, **37**, 2417761.
8 K. Sahoo, L. Juneja, R. Naik and S. Bhaumik, *Nanoscale Adv.*, 2025, **7**, 5411–5420.
9 M. R. Patel, P. Chetti, T. J. Park and S. K. Kailasa, *ACS Appl. Nano Mater.*, 2024, **7**, 22640–22649.
10 D. Li, P. Zhuang and C. Sun, *J. Mater. Chem. C*, 2024, **12**, 4544–4561.
11 C.-M. Lee, E.-H. Jeong, H.-S. Kim, S.-Y. Choi and M.-H. Park, *Materials*, 2025, **18**, 4195.
12 J. C. Dahl, E. B. Curling, M. Loipersberger, J. J. Calvin, M. Head-Gordon, E. M. Chan and A. P. Alivisatos, *ACS Nano*, 2024, **18**, 22208–22219.
13 Q.-W. Yin, J. Wang, J.-Z. Liu, J.-T. Huang, C.-K. Yang, R.-S. Li, J. Ling and Q. Cao, *Microchem. J.*, 2024, **207**, 111725.
14 M. Kazes, T. Udayabhaskararao, S. Dey and D. Oron, *Acc. Chem. Res.*, 2021, **54**, 1409–1418.
15 S. Akhil, S. Biswas, M. Palabathuni, R. Singh and N. Mishra, *J. Phys. Chem. Lett.*, 2022, **13**, 9480–9493.
16 M. Shellaiah, K. W. Sun, N. Thirumalaivasan, M. Bhushan and A. Murugan, *Sensors*, 2024, **24**, 2504.
17 S. Chatterjee, S. Biswas, S. Sourav, J. Rath, S. Akhil and N. Mishra, *J. Phys. Chem. Lett.*, 2024, **15**, 10118–10137.
18 C. Collantes, W. Teixeira, V. González-Pedro, M.-J. Bañuls, P. Quintero-Campos, S. Morais and Á. Maquieira, *Dalton Trans.*, 2023, **52**, 18464–18472.
19 H. Xia, L. Wang, H. Ding, B. Hu, Q. Li, H. Li, T. Yu, Z. Liu, F. Tian and L. Jin, *J. Alloys Compd.*, 2024, **988**, 174322.
20 Y. Jiang, J. Zhou, J. Tang, Q. Zhou, X. Zhao, Z. Teng, L. Qi and K. Pan, *Mater. Today Commun.*, 2025, **42**, 111123.
21 K. K. Chan, D. Giovanni, H. He, T. C. Sum and K.-T. Yong, *ACS Appl. Nano Mater.*, 2021, **4**, 9022–9033.
22 W. Song, Y. Wang, B. Wang, Y. Yao, W. Wang, J. Wu, Q. Shen, W. Luo and Z. Zou, *Nano Res.*, 2020, **13**, 795–801.
23 W. Song, D. Wang, J. Tian, G. Qi, M. Wu, S. Liu, T. Wang, B. Wang, Y. Yao, Z. Zou and B. Liu, *Small*, 2022, **18**, 2204763.
24 B. Shi, J. Lü, Y. Liu, Y. Xiao and C. Lü, *Mater. Chem. Front.*, 2021, **5**, 4343–4354.
25 K.-A. Shen and C.-G. Shi, *New J. Chem.*, 2021, **45**, 7225–7230.
26 J. Zhu, Z. Xie, X. Sun, S. Zhang, G. Pan, Y. Zhu, B. Dong, X. Bai, H. Zhang and H. Song, *ChemNanoMat*, 2019, **5**, 346–351.

© 2026 The Author(s). Published by the Royal Society of Chemistry

Open Access Article. Published on 02 March 2026. Downloaded on 5/3/2026 3:03:50 PM. This article is licensed under a Creative Commons Attribution-NonCommercial 3.0 Unported Licence.

27 F. Luo, S. Li, L. Cui, Y. Zu, Y. Chen, D. Huang, Z. Weng and Z. Lin, *Nanoscale*, 2021, **13**, 14297–14303.
28 S. K. Avugadda, A. Castelli, B. Dhanabalan, T. Fernandez, N. Silvestri, C. Collantes, D. Baranov, M. Imran, L. Manna, T. Pellegrino and M. P. Arciniegas, *ACS Nano*, 2022, **16**, 13657–13666.
29 Y. Asakura, S. Adiwijaya, S. Yoshino, H. Kato and Y. Yamauchi, *Adv. Sci.*, 2025, **12**, e108489.
30 H. Zhang, S. Cao, J. Jiang, Q. Sun, J. Liu, D. Ou, J. Zhao, W. Yang, H. Fu and J. Zheng, *Chem. Eng. J.*, 2023, **462**, 142330.
31 W. Zhuang, D. Yao, M. Li, W. Xu, Q. Cen, M. Zhang, H. Li, X. Yan and H. Zhang, *Sens. Actuators, B*, 2024, **416**, 136014.
32 L. De Trizio, I. Infante and L. Manna, *Acc. Chem. Res.*, 2023, **56**, 1815–1825.
33 M. A. Shuheil, G. PadmaPriya, S. Ray, T. A. Qassem, G. Garg, R. Sharma, B. Madaminov, S. Sadikova and S. Mahmoodi, *Talanta Open*, 2026, 100616.
34 J. Guan, Y. z. Shen, Y. Shu, D. Jin, Q. Xu and X. Y. Hu, *Adv. Mater. Interfaces*, 2021, **8**, 2100588.
35 M. R. Kar, U. Patel and S. Bhaumik, *Mater. Adv.*, 2022, **3**, 8629–8638.
36 Y. Miao, R. Xie, Q. Kan, Y. Yu, S. Dong, S. Wang and L. Mao, *Adv. Opt. Mater.*, 2025, **13**, 2402320.
37 G.-B. Huang, Z.-Y. Guo, T.-X. Ye, C. Zhang, Y.-M. Zhou, Q.-H. Yao and X. Chen, *J. Anal. Test.*, 2021, **5**, 3–10.
38 H. G. Li, Y. M. Zhu, X. L. Liu, Z. Y. Guo, Y. N. Huang and X. Chen, *J. Anal. Test.*, 2023, **7**, 1–7.
39 P. Zhang, C. Xiong, Z. Liu, H. Chen and S. Li, *Microchem. J.*, 2023, **190**, 108651.
40 Z. Gao, L. Ding, H. Lv, Y. Zhang, Y. Yu, S. Cheng, Y. Zong, D. Ge and S. Huang, *Appl. Surf. Sci.*, 2025, **681**, 161521.
41 H. Wang, W. Gao, Y. Li, Y. He and H. Yu, *New J. Chem.*, 2024, **48**, 11688–11696.
42 J. Chen, J. Shao, R. Sun, W. Zhang, Y. Huang, J. Zheng and Y. Chi, *Anal. Chem.*, 2023, **95**, 11839–11848.
43 R. Ma, J. Mei, J. Gan, F. Du and C. Qiu, *Microchim. Acta*, 2025, **192**, 24.
44 V. G. Vasavi Dutt, S. Akhil and N. Mishra, *ChemistrySelect*, 2021, **6**, 8171–8176.
45 M. A. R. Laskar, M. T. Rahman, K. M. Reza, A. A. Maruf, N. Ghimire, B. Logue and Q. Qiao, *J. Mater. Chem. C*, 2023, **11**, 8590–8599.
46 J. Fu, L. Zhang, S.-L. Wang, W.-L. Yuan, G.-H. Zhang, Q.-H. Zhu, H. Chen, L. He and G.-H. Tao, *J. Hazard. Mater.*, 2022, **425**, 127981.
47 M. Chen, J. An, Y. Hu, R. Chen, Y. Lyu, N. Hu, M. Luo, M. Yuan and Y. Liu, *Sens. Actuators, B*, 2020, **325**, 128809.
48 X.-H. Tan, G.-B. Huang, Z.-X. Cai, F.-M. Li, Y.-M. Zhou and M.-S. Zhang, *J. Anal. Test.*, 2021, **5**, 40–50.
49 J. Wang, Y.-L. Hu, R.-X. Zhao, Q.-L. Wen, J. Wang, N. Yang, J. Ling, C. Z. Huang and Q. Cao, *Microchem. J.*, 2021, **170**, 106769.
50 M. R. Kar, U. Patel and S. Bhaumik, *Mater. Adv.*, 2022, **3**, 8629–8638.
51 S. Bougossa, A. Guesmi, J. Wannassi, N. Mhadhbi, N. B. Hamadi, L. Khezami, J. Erwann, H. Barhoumi and H. Naïli, *J. Solid State Chem.*, 2025, **352**, 125566.
52 M. Shellaiah, L.-H. Chuang, K. Awasthi, N. Ohta and K. W. Sun, *Inorg. Chem. Commun.*, 2025, 114806.
53 Y. Li, Y. Ding, J. Sun, S. Tan, Y. Li, X. Wang, J. Cai, J. Bai, X. Lv and W. Guo, *SmartMat*, 2025, **6**, e70022.
54 Y. Li, X. Tan, S. Wu, W. Hong, J. Luo, S. Zhao, L. Sun, J. Lin, Q. Chen and M. Zhang, *Sens. Actuators, B*, 2025, **426**, 137092.
55 C.-Y. Li, M. Shellaiah and K. W. Sun, *J. Electrochem. Soc.*, 2023, **170**, 077505.

© 2026 The Author(s). Published by the Royal Society of Chemistry